

Development of order in a symmetric unstable system

Gene F. Mazenko

The James Franck Institute and the Department of Physics, The University of Chicago, Chicago, Illinois 60637

Oriol T. Valls

School of Physics and Astronomy, University of Minnesota, Minneapolis, Minnesota 55455

(Received 27 September 1982; revised manuscript received 23 February 1983)

We consider the problem of growth of order on arbitrary length scales in a thermodynamically unstable system. Starting from simple physical ideas about self-similarity, we develop a renormalization-group formalism to treat the case of an initially disordered square-lattice single spin-flip kinetic Ising model in zero field subjected to a quench to a final temperature T_F lower than the critical temperature T_c . We derive and solve recursion relations for the structure factor $\tilde{C}(\vec{q}, t)$ and for the short-range order parameter $\epsilon(1, 0; t)$. We find that $\tilde{C}(\vec{q}, t)$ has, as a function of wave number q , an approximately Gaussian peak at $q=0$ that sharpens to a δ function as the time, t , after the quench goes to infinity. This peak is associated with the growth of domains. At intermediate times the width, $q_w(t)$, decreases as $(t-t_0)^{-1/2}$. The area under the peak increases with time logarithmically at first and tends asymptotically to the square of the equilibrium magnetization. The average magnetization is zero for all finite times. At long times and small \vec{q} , scaling laws follow analytically from the recursion relations. As a function of t and of T_F , $\tilde{C}(\vec{q}, t)$ exhibits a pulse and peak structure similar to, but richer than, that previously found for quenches within the disordered phase. We discuss the relation of our results to Monte Carlo, experimental, and previous theoretical work and conclude with suggestions for improvements.

I. INTRODUCTION

There exists a variety of thermodynamically unstable systems which, though rigorously incapable of generating true long-range order, can nonetheless produce order on arbitrarily large length scales. Consider a very large system that is initially completely disordered with respect to some order parameter ψ . At some time the temperature¹ is rapidly lowered to a value below a critical temperature T_c . Suppose the system is then thermodynamically unstable with respect to two² degenerate equilibrium states. The system will immediately begin to phase separate into domains of the two competing states. The degeneracy of the two "final" states is tantamount to saying there is no external ordering field (i.e., the conjugate to the order parameter) acting on the system. Consequently the system will, strictly speaking, never be able to choose between the equilibrium states and there will never be symmetry breaking in the problem. The average value of the order parameter over an infinite system will remain zero for all times. However, as time evolves, the domains of the competing equilibrium phases grow inexorably³ larger and locally it will appear that one has long-range ordering—the longer the time the

longer the range.

Such situations are common. In a condensed-matter context there is "ordering" in the absence of an ordering field for antiferromagnets, superfluid ^4He , superconductors, and a variety of order-disorder transitions. The early evolution of the universe⁴ may also provide examples of this type. In the final analysis, for very long times, it would be virtually impossible to distinguish between true long-range order and the type of local order we discuss here.

The physical situation described above is intuitively obvious but mathematically elusive. The existing theories⁵ are not powerful enough to distinguish between the size of a domain and the range of local equilibrium correlations in a domain.⁶ These conventional approaches have difficulties treating this problem because it involves the development of order on all length scales larger than that characterizing the disordered phase and the competition and interaction between those many length scales. We now appreciate that problems involving many competing length scales are conveniently treated using⁷ renormalization-group (RG) methods. In this paper we develop such a treatment.

The particular problem we study is the sudden

temperature quench, in zero field, of a square-lattice ferromagnetic⁸ kinetic Ising (KI) model with spin-flip dynamics. We wish to treat here the case where the quench is from a high temperature T_I to a temperature T_F below the transition temperature T_c . The approach we use is a direct extension of the generalized RG methods developed recently⁹ to treat a temperature quench within the disordered region.

Our main results (see Sec. V) are that the average magnetization, for an infinite system, is zero¹⁰ for all finite times t after the quench,

$$m(t)=0, \quad (1.1)$$

and that the wave-number-dependent structure factor is given approximately, except at early times, by a scaling form

$$\tilde{C}(\vec{q}, t) = \frac{M_E^2(t)}{q_w^2(t)} f(\vec{q}/q_w(t)) + \tilde{C}(\vec{q}, T_F). \quad (1.2)$$

In (1.2) \vec{q} is the wave vector, $M_E(t)$ is an effective time-dependent magnetization, and $\tilde{C}(\vec{q}, T_F)$ is the equilibrium-structure factor associated with the temperature T_F . The function $f(\vec{x})$ is peaked about $\vec{x}=0$ (approximately a Gaussian) and its integral is unity. The width $q_w(t)$ is to be associated with the growth of domains of size $L(t)=2\pi/q_w(t)$.

As shown in Fig. 1 we find a very sharp central peak developing at $\vec{q}=0$ as time evolves. The area under this peak is given by $M_E^2(t)$, which approaches

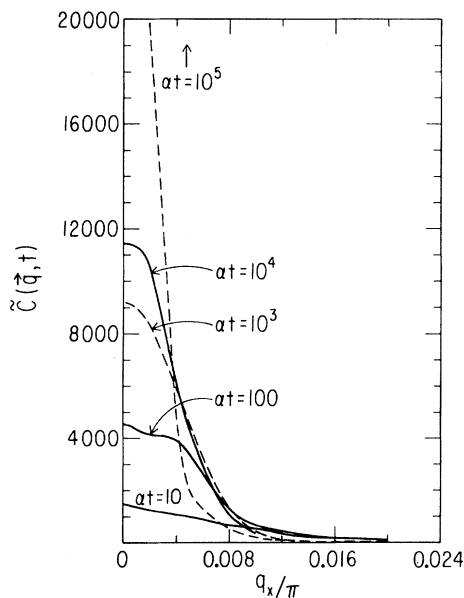


FIG. 1. Structure factor $\tilde{C}(\vec{q}, t)$ vs $q_x/\pi=q_y/\pi$ for several times, $u_F=\tanh K_F=0.42$, and $u_I=0$. The growth and progressive narrowing of the central peak can be clearly seen.

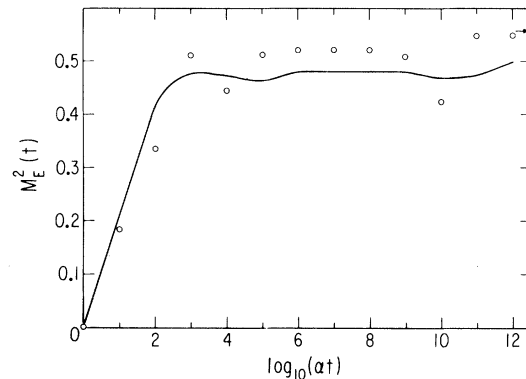


FIG. 2. Effective magnetization squared as a function of time for $u_F=0.42$. The solid line represents $M_E^2(t)$, the area under the central peak [see (5.19)], while the dots represent $M_G^2(t)$, the value obtained by assuming that the peak is Gaussian, [see (5.22)]. The arrow points to the equilibrium value of the magnetization squared

the equilibrium spontaneous magnetization squared for long times (see Fig. 2) even though for any finite time the average magnetization is zero. The width $q_w(t)$ is shown as a function of time in Fig. 3. We find that q_w decays as $(t-t_0)^{-1/2}$ for intermediate times, where t_0 is roughly associated with the time at which well defined domains appear. This is in agreement with other theoretical,^{6,11-16} Monte Carlo,¹⁷⁻¹⁹ and experimental^{20,21} results. For long times we find a crossover to a much slower decay for $q_w(t)$ going as $(\ln t)^{-1}$.

We also present results (Fig. 4) which demonstrate

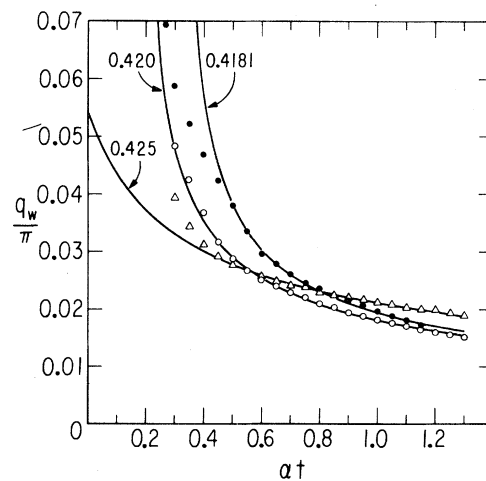


FIG. 3. Width of the central peak vs time, for the temperatures indicated (see Sec. V). The triangles and dots are the results of our calculation, while the solid lines are fits to the form $q_w/\pi = \beta^{-1}(t-t_0)^{-1/2}$ and the values of β and t_0 for the three temperatures are given in Table II.

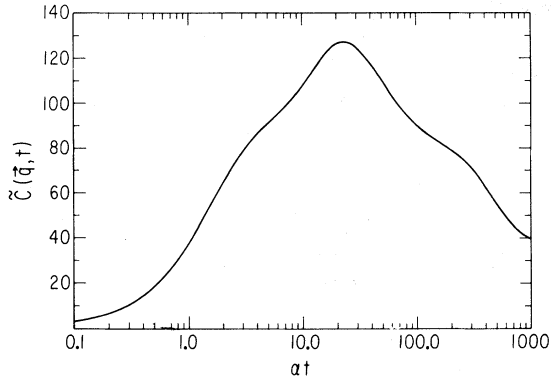


FIG. 4. Structure factor $\tilde{C}(\vec{q}, t)$ as a function of time for $q_x/\pi = q_y/\pi = 0.02$ and $u_F = 0.42$. The equilibrium value is approximately 18.

the existence of a “pulse” structure at finite wave numbers. This structure was previously found, in a simpler form, in one dimension²² and in paper I.⁹ Similarly, we look at the dependence of $\tilde{C}(\vec{q}, t)$ on the final temperature T_F for fixed wave number and find two peaks (see Fig. 5) for long times. The peak for $T_F > T_c$ was obtained in I, and there is now also a peak for $T_F < T_c$.

We believe that our approximate calculation leads to a good qualitative description of this system with quantitative reliability in the short and intermediate time regimes. There are, however, some aspects of the calculation which oversimplify the problem and lead to implausible very-long-time freezing and un-freezing behaviors. We will discuss this behavior and the reasons for it in Sec. VI.

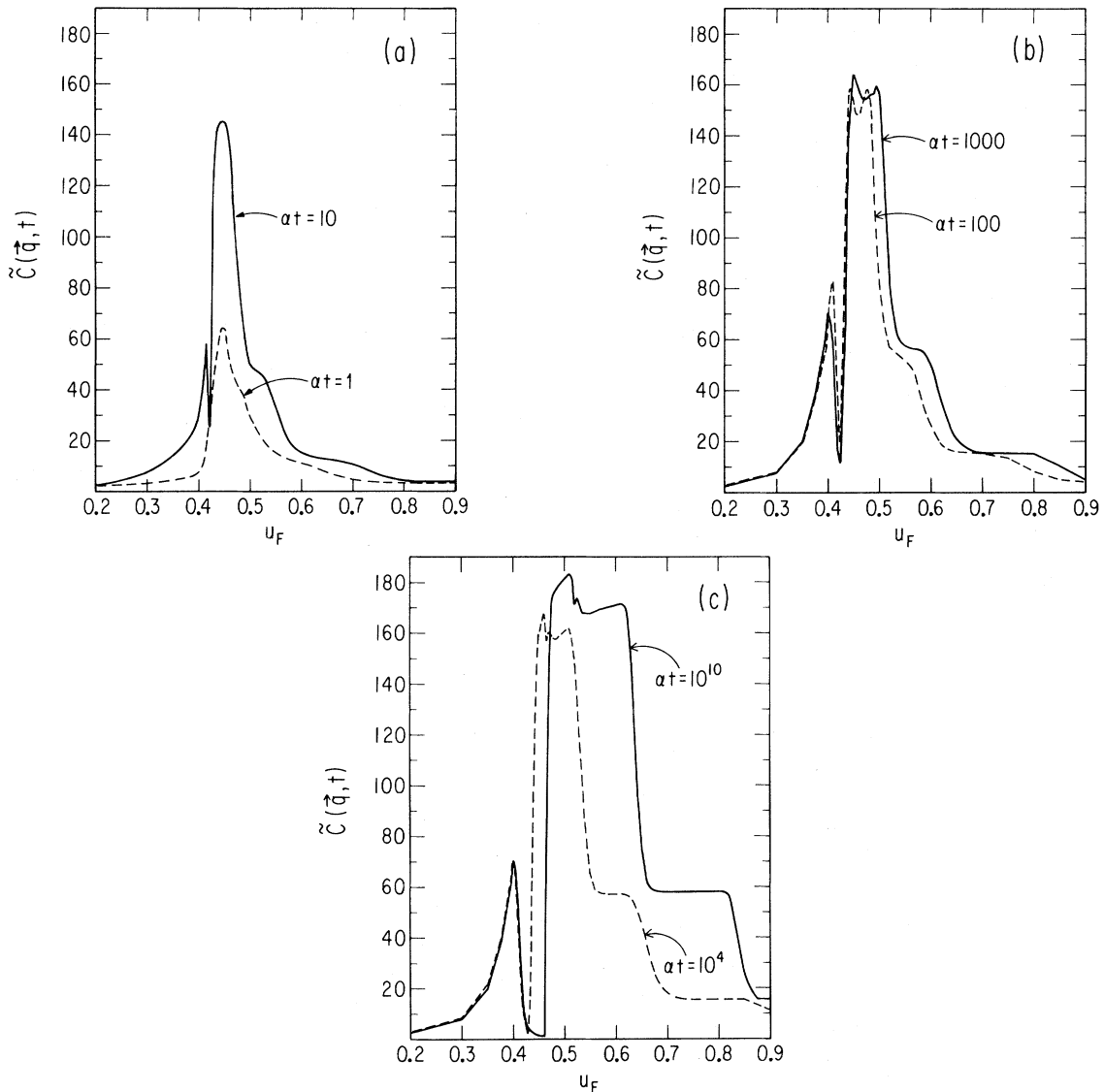


FIG. 5. $\tilde{C}(\vec{q}, t)$ vs u_F , at times indicated for $9x/\pi = 9y/\pi = 0.03$.

In the next section we define our problem more carefully and discuss related work. We follow this in Sec. III with a qualitative discussion which we believe physically motivates the use of a RG treatment in this problem. The key aspect here is the development of domains on arbitrary length scales and the existence of a self-similarity in the problem connecting different length and time scales. This self-similarity can be exploited by developing recursion relations connecting problems on these different time and length scales. We indicate how these recursion relations lead to a solution of the problem.

In Sec. IV we recapitulate the RG method introduced in paper I and discuss the rather involved derivation of the main mathematical result of this paper: the recursion relation satisfied by the structure factor $\tilde{C}(\vec{q}, t)$. Those not interested in these details can jump to Sec. V where we present the results of the solution of the recursion relation for $\tilde{C}(\vec{q}, t)$. In the final section we discuss the limitations of these results and speculate on how they can be improved.

II. BACKGROUND AND MODEL STUDIED

The problem we study here is the simplest among a family of problems occurring in magnetic, solid, and fluid systems. We should differentiate between systems where the order parameter is conserved (fluids, and some ferromagnetic systems) and those where it is not (antiferromagnets, superfluid helium, superconductors, order-disorder transitions in alloys). We must also differentiate between systems where the conjugate field is externally adjustable (e.g., ferromagnets) and those where it is not (e.g., antiferromagnets, fluids). Finally, there can be couplings to auxiliary fields which may play a major role in describing the dynamics in a system (as in the coupling to flow via the velocity field in a fluid). We study the case of a nonconserved order parameter, in zero external field, and in the absence of mode coupling effects.

A physically relevant situation is the ordering of an alloy after a temperature quench. Hashimoto *et al.*²⁰ have carried out such experiments in Cu₃Au and have followed the evolution of the structure factor $\tilde{C}(\vec{q}, t)$ using x-ray scattering. There is good qualitative agreement between their experiments and our results. They find a growing central peak with a width decreasing in time as $(t - t_0)^{-1/2}$.

There are several theoretical models which are believed to be appropriate to this problem. The simplest field theoretical model describing an ordering process with a nonconserved order parameter is the relaxational time-dependent Ginzburg-Landau (TDGL) model.²³ The conserved order-parameter

counterpart of this model has been studied extensively²⁴ since it models the problem of spinodal decomposition. This problem differs significantly from the one we have studied because of the conservation law satisfied by the order parameter. If the wave-number-dependent order parameter ψ_q is conserved, then $\psi_{q=0}$ does not change with time. This means that the $q=0$ component of $\langle |\psi_q|^2 \rangle$ is pinned at its initial high-temperature value. This forces $\langle |\psi_q|^2 \rangle$ to be peaked as a function of q for times after the quench.

A more realistic description of our problem is given by an antiferromagnetic spin-exchange kinetic Ising (ASEKI) model.²⁵ In this model the concentration or, in magnetic language, the magnetization $m = \psi_{q=0}$ is conserved. The ordering in these systems is, however, at a finite wave number \vec{q}_0 and the order parameter is the staggered magnetization $\psi_{\vec{q}_0}$ which is not conserved.

One can construct a model somewhat simpler than the spin-exchange model if one neglects the influence of m on $\psi_{\vec{q}_0}$. This is the single spin-flip kinetic Ising (SFKI) model²⁶ (defined below). For wave vectors near \vec{q}_0 , it should be very similar to the ASEKI model. Finally, we note⁸ that an antiferromagnetic square lattice with $\vec{q}_0 = (\pi, \pi)$ (in units of the inverse lattice constant) is equivalent to the ferromagnetic SFKI ($\vec{q}_0 = 0$) which we consider in this work.

There has been theoretical and numerical work on all three models listed above. Billotet and Binder⁶ have studied the TDGL model in three dimensions by using the method of Langer, Bar-on, and Miller²⁴ (which had been developed for the case of a conserved order parameter.) They found that this method leads to a time-dependent structure factor of the form [see Eq. (89) in Ref. 6]

$$\tilde{C}(\vec{q}, t) = \tilde{C}(\vec{q} = 0, T_F) \left[\frac{q_{\max}}{q} \right]^2 \times [1 + f(t)\tilde{S}(\vec{q}t^{1/2})]. \quad (2.1)$$

This clearly has an unphysical wave-number dependence for small wave numbers. As they point out, their result is incompatible with expectations, based on physical grounds, that $\tilde{C}(\vec{q}, t)$ should be composed at long times of two peaks, centered at $q=0$, with widths associated with two lengths: the correlation length ξ and the domain size L . At late times $L \gg \xi$. They conclude that in their “theory as well as in Langer’s theory of spinodal decomposition, there is room for one effective length” only and these theories describe “only the initial stages of the

nonlinear relaxation process" where no domains larger than ξ exist. Therefore their theory "as well as Langer's theory are incapable of correctly describing the decay of metastable states."

Kawasaki, Yalabik, and Gunton¹¹ also treat a TDGL model. In some sense their calculation goes in the opposite direction to that of Ref. 6. While they also obtain a single length it is to be associated with the growth of domains. Since they ignore the effects of thermal noise, finite wave numbers never properly equilibrate and the correlation length does not appear in their calculation. After a series of rather drastic approximations they obtain the result that the width of their central peak decreases, for very long times, as $t^{-1/2}$.

A phenomenological but very physical approach to the long-time behavior in this system and a TDGL model involves the assumption that the main dynamical mechanism after local equilibrium is established is via the motion of domain walls. Allen and Cahn¹² have shown¹³ in this case that the average domain size L grows as $(t-t_0)^{1/2}$ and found some experimental support²¹ for their result from direct observation of individual domain growth. Subsequent theoretical investigations¹⁴⁻¹⁶ along the same lines support these conclusions.

Kawabata and Kawasaki¹⁷ have carried out a Monte Carlo study of the SFKI model (with a slightly different flipping probability²⁷ than we treat here). Qualitatively the structure factor they obtain after a quench from infinite temperature down to $T_F=0.2T_c$ is in agreement with the results we find here and are observed in experiment. They find a central peak sharpening about $\vec{q}=0$ as time proceeds and see a pulslike behavior for fixed \vec{q} as a function of time. They also find a width for the central peak which "seems" to vary as $t^{-1/2}$ for the longest times they treat.

There is, however, an obvious problem with the Monte Carlo results in Ref. 17 since they obtain a nonzero value for the average magnetization at finite times. This is a consequence of working with a finite (40×40 sites) system. If one repeats the calculation of $m(t)$ in Ref. 17 using a larger system ($N \times N$) one finds²⁸ that the average magnetization, $m_N(t)$, again approaches its equilibrium value, but at a time which increases sharply with N . This leads to the result $m_{40}(t) > m_N(t)$. Clearly this implies that in the thermodynamic limit $m(t)=0$. For any finite system, a single domain will eventually engulf the system, but in an infinite system there is always an equal distribution of "up" and "down" domains. Hence, it is necessary to check carefully the size dependence of $\tilde{C}(q,t)$ in a Monte Carlo calculation before interpreting the results.

More careful Monte Carlo studies of the ASEKI

model have been carried out in three¹⁸ and two dimensions.¹⁹ These studies, which can only be carried out for limited time ranges and with a coarse wave-number resolution, lead to conclusions completely compatible with those we find here. They show in both two and three dimensions that there is approximate scaling of the form given by (1.2) with $M_E^2(t)$ taking its asymptotic value and $q_w(t) \sim (t-t_0)^{-1/2}$ for intermediate times.

As explained above we study here the SFKI model on a square lattice. It is very convenient to study this model: Some of the equilibrium quantities, such as the magnetization m and the nearest-neighbor correlation function $\epsilon(0,1)$ are known exactly^{29,30} as a function of temperature, and the equilibrium structure factor $\tilde{C}(\vec{q},T)$ has been studied by series methods.³¹⁻³³ Moreover, we have previously obtained excellent agreement with many known results when we have calculated m and^{34,35} $\tilde{C}(\vec{q},T)$ (as well as dynamic fluctuations in equilibrium) using the same real-space renormalization methods which were extended in I to time-dependent problems. We recall that the SFKI model (or a relatively simple variant) serves as a reasonable first approximation for the dynamics of a number of systems including certain antiferromagnetic systems³⁶ and the order-disorder process of some binary alloys.³⁷

In detail, the model that we study here is precisely that studied in Refs. 34 and 35, and in I. Therefore, we merely recall here some definitions in order to introduce notation: Consider a set of N classical spin- $\frac{1}{2}$ Ising spins $\{\sigma\}$ located at sites \vec{r}_i on a square lattice with spacing c . In thermal equilibrium, at a temperature T , the probability distribution governing these spins is

$$P[\sigma, K] = \exp(H[\sigma, K]) / Z(K), \quad (2.2)$$

where $H[\sigma, K]$ is the nearest-neighbor Ising Hamiltonian characterized by a positive coupling $K = J/k_B T$, J is the exchange constant, and $Z(K)$ is the partition function.

We assume that the dynamics of the Ising spins³⁸ are driven by a heat bath via a single spin-flip operator (SFO) $D_\sigma(K)$ which depends on the temperature of the bath and is given by

$$D[\sigma | \sigma'; K] = -\frac{\alpha}{2} \sum_i \Lambda_{\sigma, \sigma'}^{[i]} W_i[\sigma', K] \sigma_i \sigma'_i, \quad (2.3)$$

where α is a flipping rate,

$$\Lambda_{\sigma, \sigma'}^{[i]} = \prod_{k(\neq i)} \delta_{\sigma_k, \sigma'_k} \quad (2.4)$$

tells us that the matrix $D[\sigma | \sigma'; K]$ is almost diagonal, and we choose the spin-flip probability to be

$$W_i[\sigma, K] = 1 - \frac{a(K)}{2} \sigma_i \sum_a \sigma_{i+\delta_a} + \frac{a^2(K)}{4} \sum_a \sigma_{i+\delta_a} \sigma_{i+\delta_{a+1}}, \quad (2.5)$$

with

$$a(K) = \tanh(2K). \quad (2.6)$$

The δ_a in (2.5) are the vectors connecting a site to its four nearest neighbors. Thermal equilibrium between the bath and Ising spins requires that $P[\sigma, K]$ be invariant under time translations generated by $D_\sigma(K)$,

$$e^{D_\sigma(K)t} P[\sigma, K] = P[\sigma, K], \quad (2.7)$$

and this condition requires that $a(K)$ in (2.5) be given by (2.6).

All times are measured in units of the inverse flipping rate α^{-1} , which can vary drastically depending on the specific problem under consideration. α^{-1} may range from as low as 10^{-12} sec in some magnets³⁶ to hours (e.g., in the case of binary alloys³⁷ where it is primarily determined by solid-on-solid diffusion times which are very long). Hence, the time domain of physical interest may be extremely different for different problems. When we use expressions such as "early time" we mean αt small, but such times correspond to widely different physical times. While we assume that α is temperature independent, as in Monte Carlo studies, this is clearly unrealistic if one investigates a wide range of temperatures. In comparing with experiment in detail³⁹ one must take this temperature dependence into account.

Suppose we rapidly change the temperature of the bath from T_I to T_F . We assume, in keeping with Monte Carlo studies⁴⁰ of this problem, that this quench is instantaneous. The Ising system will respond to this quench through its dynamic coupling to the bath via the SFO $D_\sigma(K_F)$ which drives the Ising system to equilibrium with the bath at temperature T_F . The probability distribution governing the Ising spins for times $t \geq 0$ is given by

$$P[\sigma, t] = \exp[tD_\sigma(K_F)]P[\sigma, K_I]. \quad (2.8)$$

The nonequilibrium quantities of interest are the magnetization,

$$m(t) = \frac{1}{N} \sum_i \sum_\sigma \sigma_i P[\sigma, t], \quad (2.9)$$

the nearest-neighbor correlation function,

$$\epsilon(1, 0; t) = \frac{1}{4N} \sum_{i,a} \sum_\sigma \sigma_i \sigma_{i+\delta_a} P[\sigma, t], \quad (2.10)$$

and, finally, the structure factor,

$$\tilde{C}(\vec{q}, t) = \frac{1}{M} \sum_{i,j} e^{i\vec{q} \cdot (\vec{r}_i - \vec{r}_j)} \sum_\sigma \sigma_i \sigma_j P[\sigma, t]. \quad (2.11)$$

We shall focus our efforts on the calculation of $\tilde{C}(\vec{q}, t)$. First, however, we want to discuss some important qualitative features of the present problem.

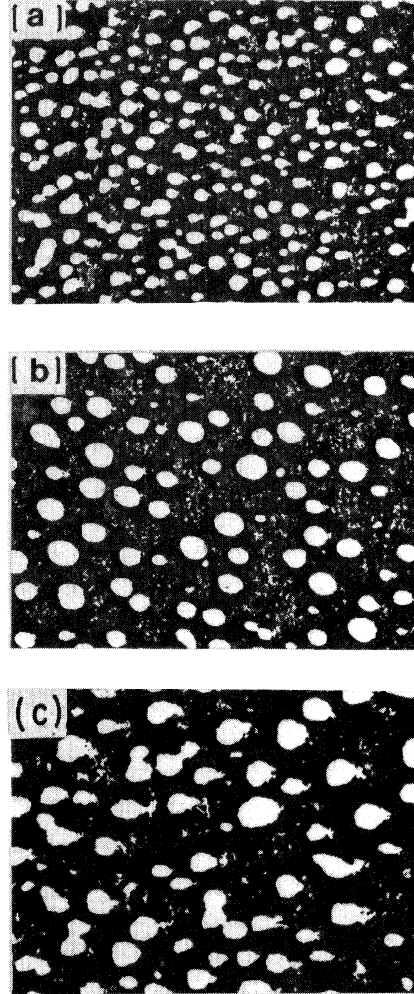


FIG. 6. Domain structures imaged (Ref. 41) with B_2 superlattice reflection in 23.0 at. % Al in Fe alloy. The samples were quenched from 630°C and annealed at 570°C. In panel (a) the system was annealed for 100 min while in panel (b) it was annealed for 1000 min. In panel (c) we have taken a portion of panel (a) with approximately the same number of domains as in panel (b) and then blown this portion up to the same size as panels (a) and (b). Comparison of panels (b) and (c) illustrates the self-similar structure of the system under simultaneous rescaling of space and time.

III. QUALITATIVE DESCRIPTION OF APPROACH

Before discussing the formal aspects of this problem in the next section it is useful to consider the basic physics involved in a qualitative and intuitive way. At some early time t_1 , after the quench, some ordered regions, domains, or droplets, will have started to form [see Fig. 6(a)].⁴¹ At some later time $t_2 > t_1$ the ordered regions will, of course, have grown in size [Fig. 6(b)]. If we call l_1 the characteristic size of these domains at time t_1 , then at t_2 we have $l_2 > l_1$. If we wait long enough all length scales larger than a lattice spacing enter the problem. We also notice that structures on a given scale are built up from structures from a smaller scale so that the various scales interact. This interaction between arbitrarily large length scales is the ingredient which makes this problem difficult. An observable such as $\tilde{C}(\vec{q}, t)$ will have contributions from all length scales as time evolves and, in order to calculate it, we must be able to treat the interaction between scales. In general we do not know how to deal with such problems. The following physical observation leads to hope.

Imagine that we begin, right after the quench, observing the system with a spatial resolution ΔL_1 . After a while we will note, at time t_1 , the appearance of domains. Let us now decrease the resolving power of our "microscope" to $\Delta L_2 > \Delta L_1$. Then, we shall not be able to observe domains until a time $t_2 > t_1$, at which time, however, the system will look very much as at time t_1 under resolving power ΔL_1 [see Fig. 6(c)]. The system is *self-similar* if one simultaneously changes the length and time scales. Self-similarity can be conveniently exploited using RG methods.

Let us make this slightly more quantitative. If

$$\tilde{C}(\vec{q}, t, K_I, K_F) = C_0(\vec{q}, t, K_I, K_F) + P_0(\vec{q}, t, K_I, K_F) C(b\vec{q}, \Delta(K_F)t, K_I', K_F'), \quad (3.4)$$

where K_I' and K_F' are the effective couplings describing the system with the coarser resolution (or equivalently a larger lattice constant), and the time rescaling factor, $\Delta(K)$, will depend on the temperature of the bath driving the dynamics (we discuss this in detail below).

Why should one consider the establishment of such a recursion relation an advancement? The reason is that we can, as we indicate below, solve such equations rather easily by direct iteration. Let us write (3.4) schematically as

$$C^{(0)} = C_0^{(0)} + P_0^{(0)} C^{(1)}, \quad (3.5)$$

where the superscript labels the level of resolution.

we look at our system with resolution $b\Delta L$ ($b > 1$) at time t it looks qualitatively like the system viewed with resolution ΔL at an earlier time $t' = \Delta t$ ($\Delta < 1$). In the structure factor $\tilde{C}(\vec{q}, t)$, $2\pi/q$ can be associated with the resolution with which we observe the system. Our self-similarity takes the form

$$\tilde{C}(\vec{q}/b, t) \sim \tilde{C}(\vec{q}, \Delta t), \quad (3.1)$$

or letting $\vec{q} \rightarrow b\vec{q}$,

$$\tilde{C}(\vec{q}, t) \sim \tilde{C}(b\vec{q}, \Delta t). \quad (3.2)$$

Of course, one cannot expect (3.2) to be an equality. It is more realistic to write

$$\tilde{C}(\vec{q}, t) = C_0(\vec{q}, t) + P_0(\vec{q}, t) \tilde{C}(b\vec{q}, \Delta t), \quad (3.3)$$

where one should allow for overall rescaling factors such as $P_0(\vec{q}, t)$ (just as in treating critical phenomena) and for contributions like $\tilde{C}_0(\vec{q}, t)$ which come^{34,35} from short wavelengths not contained in $\tilde{C}(b\vec{q}, \Delta t)$. We assume that $\tilde{C}_0(\vec{q}, t)$ and $P_0(\vec{q}, t)$ can be obtained from a local perturbation-theory calculation that does not depend on competing length scales. Indeed we discuss in Sec. IV the derivation of (3.3), and the determination of $C_0(\vec{q}, t)$ and $P_0(\vec{q}, t)$.

There is one further point. Even though the system under resolution ΔL_1 at time t_1 may look qualitatively like the system under a coarser resolution ΔL_2 at time t_2 , the interactions between the variables characterizing the two levels may be quite different. If, as assumed in this paper, the self-similarity of the problem can be implemented via a mapping of our SFKI problem from level to level, then the interactions at the different levels will be given by just two couplings, just as K_I and K_F characterized the original problem via (2.8). Thus we really must write

We can then iterate directly and thereby connect $C^{(0)}$ to all of the various scales described by $C^{(1)}, C^{(2)}, \dots, C^{(n)}$ as follows:

$$C^{(0)} = C_0^{(0)} + P_0^{(0)} C_0^{(1)} + P_0^{(0)} P_0^{(1)} C_0^{(2)} + \dots + P_0^{(0)} P_0^{(1)} \dots P_0^{(n-1)} C^{(n)} \quad (3.6)$$

and

$$C^{(n)} = C(b^n \vec{q}, B^{(n)} t, K_I^{(n)}, K_F^{(n)}), \quad (3.7)$$

where

$$B^{(n)} = \Delta(K_F^{(n-1)}) \Delta(K_F^{(n-2)}) \dots \Delta(K_F^{(0)}). \quad (3.8)$$

A key point in our development then is the determination of the thermal recursion relation

$K' = K'(K)$, which controls the flows of the couplings K_I and K_F and the time rescaling factor $\Delta(K_F)$. The thermal recursion relation we use (for a spatial rescaling factor of $b=2$) is discussed in Ref. 42 and takes the form

$$\phi' = \phi^2, \quad (3.9)$$

where $\phi = e^{2K} \tanh K$. This recursion relation leads to the correct exponential decay of correlation functions at large distances in both the ordered and disordered phases,^{42,43} its nontrivial fixed-point solution gives the exact transition temperature for this problem,

$$u_c = \tanh K_c = (2^{1/2} - 1),$$

and leads to the exact value for the thermal critical index ($\nu=1$).

There are two stages in the determination of the time rescaling factor. The first stage involves showing that the problem is dynamically self-similar. That is, within the perturbation theory described in Ref. 34 and in the next section, that the dynamics for a system with twice the original lattice spacing is of the same form as for the original problem except that it has a renormalized flipping rate α' which is, by definition

$$\alpha' = \Delta \alpha. \quad (3.10)$$

The explicit determination of $\Delta = \Delta(K)$ follows from an analysis of the equilibrium-averaged dynamic structure factor. Since this is a rather important and delicate step, we discuss the analysis in Appendix A leading to the result

$$\Delta = 4\nu_1^2 \left[\frac{\chi(K')}{\chi(K)} \right]^2 \frac{\Gamma^{(s)}(K)}{\Gamma^{(s)}(K')}, \quad (3.11)$$

where ν_1 is related to the projection of a single spin onto a block-spin variable and is given explicitly by

$$(\nu_1)^2 = \frac{1}{2} \frac{(1+a_0)}{(2-a_0^2)}, \quad (3.12)$$

where

$$a_0 = \tanh(2K_0), \quad (3.13)$$

and $K_0 = K_0(K)$ is the effective coupling in a cell of four spins and is given in Ref. 34 [Eq. (2.60) and Fig. 1]. As a first approximation $K_0 \sim 2K$. The quantity $\chi(K)$ in (3.11) is the magnetic susceptibility and its determination as a function of K is discussed in the next section. Finally the quantity $\Gamma^{(s)}(K)$ is the equilibrium average of the flipping probability and can be evaluated exactly, as explained in Refs. 35 and 42, in terms of the short-range correlation functions $\epsilon(1,0)$ and $\epsilon(1,1)$ which are defined by

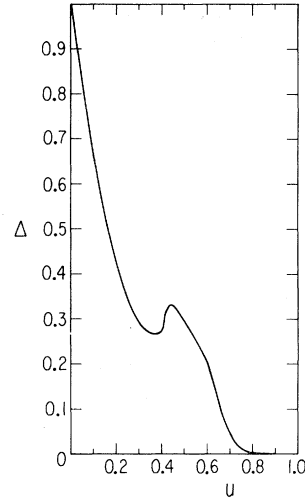


FIG. 7. Time rescaling factor Δ vs u .

$$\epsilon(m,n) = \sum_{\sigma} P[\sigma, K] \sigma_i \sigma_{i+m\hat{x}+n\hat{y}}. \quad (3.14)$$

We plot Δ vs $u \equiv \tanh K$ in Fig. 7. In the high-temperature limit $4\nu_1^2 \rightarrow 1$ and we obtain $\Delta(0)=1$ as expected. In the low-temperature limit $\nu_1 \rightarrow 1$, $x \sim y^2$ where $y = e^{-4K}$ and $\Gamma^{(s)} \sim y^2$. Since $y' = y^2$ for large enough K , we obtain

$$\Delta = 4y^2 \quad (3.15)$$

for low temperatures. It will turn out to be very important that Δ goes to zero as $K_F \rightarrow \infty$.

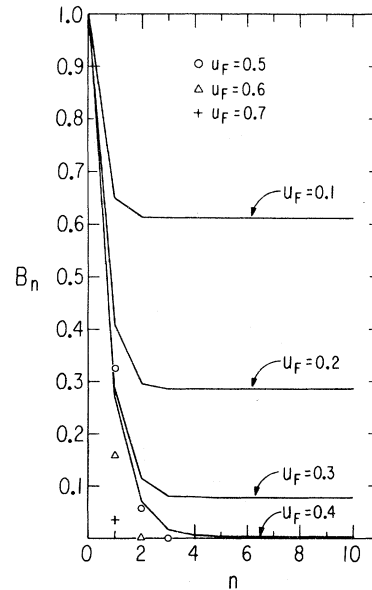


FIG. 8. Factor relating iterated and initial times [see (3.16) and (3.17)] as a function of iteration number for the indicated values of u_F .

We can now return to our iterated equation for $\tilde{C}(\vec{q}, t)$ given by (3.6) and follow the flows of the parameters under iteration. When we quench from some $K_I < K_c$ to a $K_F > K_c$ we find, under iteration, that $K_I^{(n)} \rightarrow 0$ and $K_F^{(n)} \rightarrow \infty$. Thus the problem flows to one corresponding to quenches from infinite temperature to zero temperature. The main point, however, is that the effective time

$$t^{(n)} = \Delta(K_F^{(n-1)})t^{(n-1)} \quad (3.16)$$

$$= B_n(K_F)t \quad (3.17)$$

renormalizes, after a sufficient number of iterations (see Fig. 8) to zero,

$$\lim_{n \rightarrow \infty} t^{(n)} = 0. \quad (3.18)$$

With the results developed above, we find

$$\lim_{n \rightarrow \infty} \tilde{C}(b^n \vec{q}, t^{(n)}, K_I^{(n)}, K_F^{(n)}) = \tilde{C}(\vec{q} = \infty, 0, 0, \infty), \quad (3.19)$$

and, for $t=0$, the system has not yet felt the effects of the quench, so

$$\begin{aligned} \tilde{C}(\vec{q} = \infty, t=0, K_I=0, K_F = \infty) \\ = \tilde{C}(\vec{q} = \infty, K_I=0). \end{aligned} \quad (3.20)$$

However, for $K_I=0$,

$$\tilde{C}(\vec{q}, K_I=0) = 1, \quad (3.21)$$

and, returning to the shorthand notation of (3.6),

$$\lim_{n \rightarrow \infty} \tilde{C}^{(n)} = 1. \quad (3.22)$$

From a practical point of view $\tilde{C}^{(n)}$ approaches 1 rather rapidly as a function of n and the iterated series (3.6) can then be terminated.

The original physics which motivated this RG approach enters if one notes that as time is increased it will take progressively more iterations before the system "flows" to the high-temperature fixed point. Consequently if one "waits long enough" (if t is large enough) one will obtain contributions from all scales. We see that, for t large, there will be two regimes. Initially as $K_F^{(n)}$ increases and $t^{(n)}$ is still large, one will pick up, iteratively, contributions from near the low-temperature fixed point, but, eventually, $t^{(n)}$ will be small and the high-temperature fixed-point character will completely dominate. For short times, the first regime will be brief or nonexistent. When quenching to a temperature just above or below T_c , contributions from the nontrivial fixed point will obviously control the first few iterations.

One immediate consequence of the ultimate flow to the high-temperature fixed point is that the magnetization remains zero at all finite times. The re-

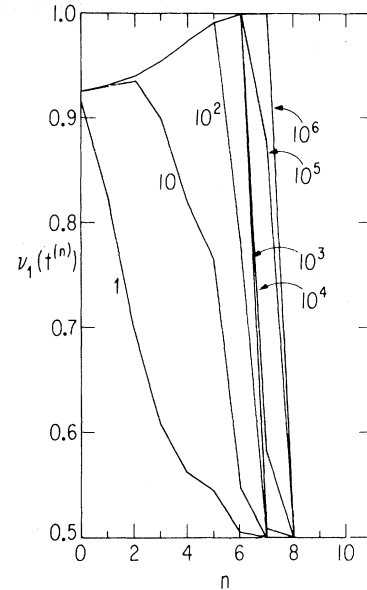


FIG. 9. Quantity $v_1(t^{(n)})$ [see (4.7)] as a function of iteration number n . The curves are labeled by the initial values of αt .

cursion relation for the magnetization is given at zeroth order by (4.4) below. Iteration of (4.4) leads eventually to multiplying by factors of v_1 [given by (4.7)] evaluated at every early times and high temperatures. In this limit $v_1 = \frac{1}{2}$ and one is led to the result (1.1). This behavior is demonstrated in Fig. 9 where we plot $v_1(t)$ for various times as a function of level of iteration. In concluding this section we hope to have convinced the reader that a RG treatment of the type described above is capable of treating the physics in this problem.

IV. RECURSION RELATION FOR $\tilde{C}(\vec{q}, t)$

The purpose of this section is to show that the assumption of self-similarity proposed in the last section can be justified mathematically and to indicate how a recursion relation of the form (3.3) can be derived. The formal aspects of developing an RG method for treating this problem are discussed in detail in paper I. We will not repeat the analysis developed there and will freely refer to equations and development in that paper and in Refs. 34 and 35.

A key aspect of our RG analysis is the development of a well-defined prescription for determining the nonequilibrium mapping function $T[\mu | \sigma; t]$. In particular we demand that $T[\mu | \sigma; t]$ be constructed using (I.4.5) and (I.4.6) such that (I.4.2) and (I.4.3) are satisfied. We then expect that $T[u | \sigma; t]$ will reduce to the appropriate equilibrium quantities,

$$T[\mu | \sigma; t=0] = T[\mu | \sigma; K_I] \quad (4.1)$$

and

$$T[\mu | \sigma; t=\infty] = T[\mu | \sigma; K_F], \quad (4.2)$$

where $T[\mu | \sigma; K]$ satisfies the eigenvalue equation^{38,44}

$$D_\sigma(K)T[\mu | \sigma; K] = D_\mu(K')T[\mu | \sigma; K], \quad (4.3)$$

where D_μ is the renormalized SFO governing the dynamics of the block spins $\{\mu\}$. $T[\mu | \sigma; t]$ is constructed in an expansion treating the effective interaction between cells as a small parameter.^{34,35} This was carried out to zeroth order in I. The result for $T^\circ[\mu | \sigma; t]$ is given by (I.4.22). Following the steps outlined below (I.4.10) one can then construct zeroth-order recursion relations for various quantities. The recursion relation for the magnetization, defined by (2.9), is

$$m(t) = v_1(t)m'(t'). \quad (4.4)$$

The nearest-neighbor correlation function $\epsilon(1,0;t)$, defined by (2.10), can easily be shown, using (I.4.34), to satisfy the zeroth-order recursion relation,

$$\epsilon(1,0;t) = \frac{r(t)}{2} + \frac{v_1^2(t)}{2}\epsilon'(1,0;t'). \quad (4.5)$$

Finally the structure factor, defined by (2.11), satisfies the zeroth-order recursion relation

$$\begin{aligned} \tilde{C}(\vec{q}, t) &= 1 + 2r(t)g_1(\vec{q}) + s(t)g_2(\vec{q}) - v_1^2(t)f(\vec{q}) \\ &\quad + v_1^2(t)f(\vec{q})\tilde{C}'(2\vec{q}, t'). \end{aligned} \quad (4.6)$$

In (4.4)–(4.6) $r(t)$ and $s(t)$ are the zeroth-order nearest- and next-nearest-neighbor correlation functions, (I.4.24), which are given explicitly in Appendix B. We also have

$$4v_1^2(t) = 1 + 2r(t) + s(t), \quad (4.7)$$

and

$$g_1(\vec{q}) = \frac{1}{2}[\cos(q_y c) + \cos(q_x c)], \quad (4.8)$$

$$g_2(\vec{q}) = \cos(q_x c)\cos(q_y c), \quad (4.9)$$

$$f(\vec{q}) = 1 + 2g_1(\vec{q}) + g_2(\vec{q}). \quad (4.10)$$

Note that (4.6) is of the form given by (3.4) with explicit expressions for C_0 and P_0 .

In this paper we extend this calculation of C_0 and P_0 to first order in the coupling between cells. We have carried out this first-order calculation for two reasons.

(i) The zeroth-order calculation is not a very severe test of the assumption that $P[\mu, t]$, defined by (I.4.1), is “similar” to $P[\sigma, t]$ (alternatively, that the

quantity $R[\mu, t]$, defined by (I.4.9), is well behaved). Also, it is not completely obvious that $T[\mu | \sigma; t]$, when constructed to higher orders, will reduce to the appropriate equilibrium forms for $t=0$ or ∞ . A first-order calculation elucidates these points.

(ii) The zeroth-order recursion relations are perfectly adequate for the study of quenching in the disordered phase (see I). The situation is different for the case of quenching into the ordered phase. We pointed out earlier^{45,35} that the zeroth-order theory fails, in the equilibrium case, to give correct results for $\tilde{C}(\vec{q}, T)$ for $T < T_c$, giving either zero or infinity for the susceptibility and a negative correlation length squared. In Ref. 45 we showed, for ordered systems, how one can treat this difficulty. However, the symmetry-breaking mechanism introduced in Ref. 45 is inappropriate to the present case where one does not have true ordering. A result of this paper is that this problem can be handled by simply going to first order in perturbation theory.

We must briefly discuss the first-order calculation for the equilibrium case which has not been discussed elsewhere. The first step in this analysis is the solution of the eigenvalue equation (4.3) with the constraints

$$\sum_\mu T[\mu | \sigma; K] = 1 \quad (4.11)$$

and

$$\begin{aligned} \sum_\sigma P[\sigma, K]T[\mu | \sigma; K] &= T[\mu' | \sigma; K] \\ &= \delta_{\mu, \mu'} P[\mu, K']. \end{aligned} \quad (4.12)$$

These equations are solved using a perturbation theory³⁴ which treats effective coupling between cells, a^R , as a small parameter. The determination of the effective coupling a_0 in a cell was discussed in Sec. III. The determination of the parameter a_R essentially⁴⁶ involves the requirement that the thermal recursion relation for K' derived from the perturbation-theory calculation agree with (3.9).

The next step, after constructing the renormalized probability distribution $P[\mu, K]$, the SFO, $D_\mu(K')$, and mapping function $T[\mu | \sigma; K]$, is to construct to first order the collective variable⁴² associated with the physical quantities of interest. These include the collective variable associated with the total spin $\sum_i \sigma_i$ and the coarse-grained variable corresponding to $\sigma_{i,a}\sigma_{j,a'}$. Averaging over the appropriate probability distributions one obtains the first-order recursion relations for the magnetization and (after Fourier transform), the static structure factor. These have the same form as at zeroth order (see I), only the coefficients are different. A key point here is that the corrections in these coefficients to the zeroth-order results are proportional to a_R .

TABLE I. The critical indices ν , β , and γ as given by the zeroth- and first-order RG calculations and compared with the exact results.

	ν	β	γ
0 order	1	0.1199	1.758
1 order	1	0.1245	1.753
Exact	1	0.125	1.75

which is not a small parameter since it ranges between 0 and 1 for $0 < K < 1$. However, a_R always appears in these expansions for the recursion relations for observables in the form $a_R(1-a_0)$. The effective expansion parameter⁴⁷ is therefore not a_R but $a_R(1-a_0)$, which is small (< 0.065) for all temperatures.

As a check on these first-order results we have calculated several static quantities. The zeroth-order result for $\epsilon(1,1)$, the next-nearest-neighbor correlation function, at T_c is 0.6199, the first-order result is 0.6279, and the exact result is 0.6366. The critical exponents are listed in Table I. In all cases there is improvement at first order.

In Fig. 10 we show the results for the magnetization, in Fig. 11 we plot the susceptibility, and in Fig. 12 we plot the static structure $\tilde{C}(\vec{q}, K)$ for $u = 0.42$ and 0.5. Analysis of these results shows that at first order there is definite improvement over the

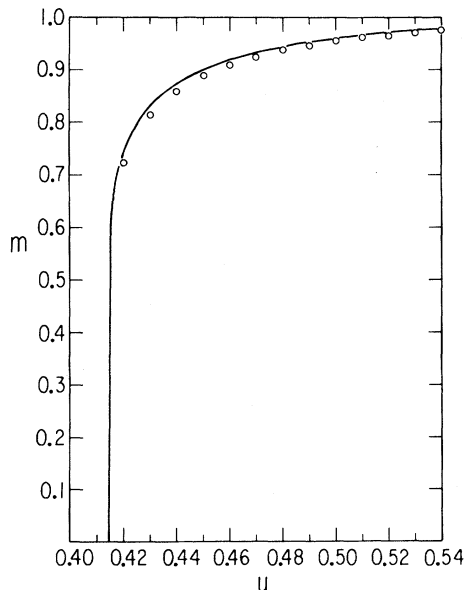


FIG. 10. Equilibrium magnetization vs u . The solid line is the first-order result and the open circles are the exact results.

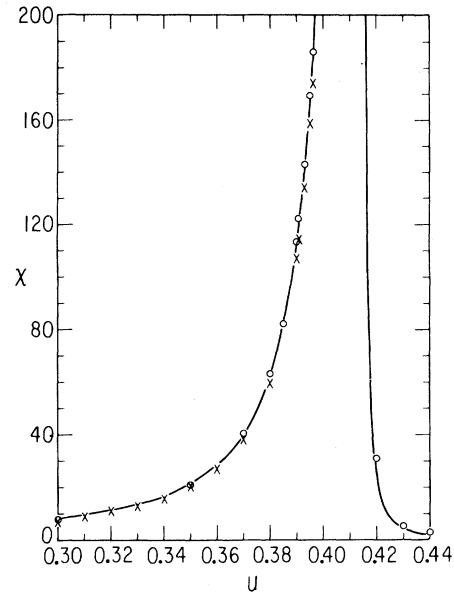


FIG. 11. Equilibrium susceptibility vs u . The solid line is the first-order result. The crosses correspond to the zeroth-order result and the circles correspond to the series results of Refs. 32 and 33.

zeroth-order result and that we have a very good description of the equilibrium state.

The general procedure to be followed in the non-equilibrium case is outlined in I below (I.4.10). Since this is an extremely involved calculation, we shall only indicate the main features here (additional details are available upon request).

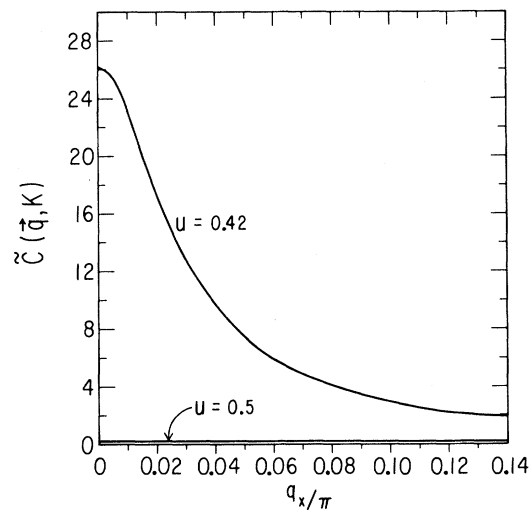


FIG. 12. The equilibrium structure factor vs $q_x = q_y$ at the values of u indicated on the figure. Note that $u = 0.42$ is the value that we have chosen for u_F in presenting many of our nonequilibrium results.

After constructing $T[\mu | \sigma; t]$ to first order we obtain the probability distribution $P[\mu, t]$ governing the block spins. We would obtain complete self-similarity if $P[\mu, t]$ is equal to

$$\bar{P}[\mu, t] = e^{D_\mu(K_F)t} P[\mu, K'_F]. \quad (4.13)$$

They are not identical and we can analyze the difference by defining a quantity $R[\mu, t]$ via

$$P[\mu, t] = R[\mu, t] \bar{P}[\mu, t]. \quad (4.14)$$

We construct $R[\mu, t]$ in perturbation theory and obtain

$$R[\mu, t] = 1 + \epsilon \kappa(t) \delta E[\mu] + O(\epsilon^2), \quad (4.15)$$

where $\delta E[\mu]$ is the deviation of

$$E[\mu] = \frac{1}{2} \sum_{i,a} \mu_i \mu_{i+\delta'_a} \quad (4.16)$$

from its average over $\bar{P}[\mu, t]$. We plot $\kappa(t)$ as a function of time in Fig. 13 for $u_I=0$ and $u_F=0.42$. We see that $\kappa(0)=\kappa(\infty)=0$, and $\kappa(t)$ is small at all times. Thus, $R \approx 1$ and the self-similarity assumption appears to be well satisfied. We will return to this point in Sec. VI.

The derivation of the recursion relation for $\tilde{C}(\vec{q}, t)$ to first order requires finding the first-order contribution to the coarse-grained variable $\pi_{i,a;j,a'}[\mu, t]$ corresponding to $\pi[\sigma] = \sigma_{i,a} \sigma_{j,a'}$ [see (I.4.7)] and then Fourier transforming. We then obtain the recursion relation for $\tilde{C}(\vec{q}, t)$ by averaging $\pi[q, \mu, t]$ with respect to $\bar{P}[\mu, t]$.

Performing all of these operations we obtain the main theoretical result of this paper, i.e., the first-order recursion relation for $\tilde{C}(\vec{q}, t)$ can be written as

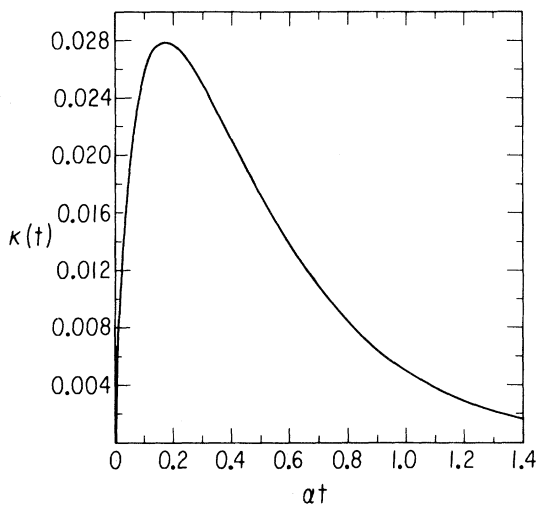


FIG. 13. Coupling $\kappa(t)$ [see (4.15)] vs αt at $u_F=0.42$.

$$\begin{aligned} \tilde{C}(\vec{q}, t) = & \tilde{C}_0(\vec{q}, t) + P_{00}(\vec{q}, t) \tilde{C}'(2\vec{q}, t') \\ & + \kappa(t) P_{01}(\vec{q}, t) H'(2\vec{q}, t'), \end{aligned} \quad (4.17)$$

which is of the form (3.4) except for a small coupling to the quantity $H(\vec{q}, t)$, which is the Fourier transform of $H_{i,a;j,a'} = \langle \sigma_{i,a} \sigma_{j,a'} \delta E[\sigma] \rangle$. This coupling is proportional, however, to the small quantity $\kappa(t)$, and, although it is not negligible (because the energy fluctuations can be large) it does not have a crucial effect on the results. One simply solves (4.17) together with the easily derived zeroth-order recursion relation for $H(\vec{q}, t)$. The explicit expressions for P_{00} , P_{01} , and C_0 to first order are very lengthy, not very illuminating, and will not be reproduced here.

At $t \rightarrow 0$ and $t \rightarrow \infty$ the recursion relation for $\tilde{C}(\vec{q}, t)$, (4.17), properly reduces to the static recursion relation at $K=K_I$ and $K=K_F$, respectively. Thus we have derived the RG equation connecting the structure factors defined with different degrees of resolution and the equations are [except for the small coupling to $H(\vec{q}, t)$] of the form proposed in the last section.

V. RESULTS

In this section we analyze the results which follow from the recursion relations derived in the last section.

A. Scaling

As shown in Fig. 1, for sufficiently long times, $\tilde{C}(\vec{q}, t)$ is a very sharply peaked function near $q=0$. This means that in the recursion relation (4.17) we can, since $\tilde{C}(q, t)$ is very large, ignore the contributions from C_0 and H and set $q=0$ and $t=\infty$ in P_{00} to obtain

$$\tilde{C}(\vec{q}, t) \approx P_{00}(0, \infty) \tilde{C}'(2\vec{q}, t'). \quad (5.1)$$

It is easy to show that

$$P_{00}(0, \infty) = P_{0,F} \quad (5.2)$$

enters the recursion relation for the magnetization corresponding to the equilibrium final state:

$$m(K_F) = \frac{1}{2} \sqrt{P_{0,F} m(K'_F)}, \quad (5.3)$$

with corrections of $O(\epsilon^2)$. This suggests that the peak contribution, $\tilde{C}_p(\vec{q}, t)$, satisfies at long times and small q , a scaling equation of the form

$$\tilde{C}_p(\vec{q}, t) = \frac{m_F^2(K_F)}{q_w^2(t)} f(\vec{q}/q_w(t)). \quad (5.4)$$

Inserting this ansatz into (5.1) and using (5.3) we obtain

$$\frac{1}{q_w^2(t)} f(\vec{q}/q_w(t)) = \frac{4}{[q'_w(t')]^2} f(2\vec{q}/q'_w(t')), \quad (5.5)$$

which is satisfied if

$$q_w(\Delta t, K_I', K_F') = 2q_w(t, K_I, K_F). \quad (5.6)$$

Such scaling relations are particularly useful if one is near a fixed point. If $K_I = K_I' = 0$ and $K_F = K_F' = K_C$, then

$$q_w(\Delta(K_C)t) = 2q_w(t), \quad (5.7)$$

which has the simple power-law solution,

$$q_w = q_c t^{-x}, \quad (5.8)$$

with

$$x = -\frac{\ln 2}{\ln \Delta(K_C)}. \quad (5.9)$$

Thus, as expected, we find dynamic scaling in this regime: Characteristic times in the problem enter as $(q_w)^z$, where z is the dynamic critical index given by the usual expression³⁵

$$z = \frac{-\ln \Delta(K_C)}{\ln 2} \equiv \frac{1}{x}. \quad (5.10)$$

If, on the other hand, we quench to $T_F \rightarrow 0$, we have the solution

$$q_w = \frac{q_0 / (\ln y^{-1})}{\ln \alpha t}, \quad (5.11)$$

with q_0 temperature independent and $y = e^{-4K}$. Thus, we find a logarithmic decay of q_w at very long times.

For wave numbers outside the peak region we expect that the system is equilibrating for long times and we can write

$$\tilde{C}(\vec{q}, t) = \tilde{C}_p(\vec{q}, t) + \tilde{C}(\vec{q}, K_F). \quad (5.12)$$

Since we have the sum rules:

$$\int \frac{d^2 q}{(2\pi)^2} \tilde{C}(\vec{q}, K_F) = 1 - m^2(K_F), \quad (5.13)$$

$$\int \frac{d^2 q}{(2\pi)^2} \tilde{C}(\vec{q}, t) = 1, \quad (5.14)$$

we easily identify, making use of (5.4),

$$\int \frac{d^2 q}{(2\pi)^2} \frac{1}{q_w^2(t)} f(\vec{q}/q_w(t)) = 1. \quad (5.15)$$

For increasing time $q_w \rightarrow 0$, $f(\infty) = 0$ and the integral (5.15) remains finite. Together these properties define a Dirac δ function,

$$\lim_{t \rightarrow \infty} \frac{1}{q_w^2(t)} f(\vec{q}/q_w(t)) = (2\pi)^2 \delta(\vec{q}), \quad (5.16)$$

and we arrive at the expected result,

$$\lim_{t \rightarrow \infty} \tilde{C}(\vec{q}, t) = m^2(K_F) \delta(\vec{q}) + \tilde{C}(\vec{q}, K_F). \quad (5.17)$$

B. The nearest-neighbor correlation function

The nonequilibrium nearest-neighbor correlation function $\epsilon(1,0;t)$, defined by (2.10), which is¹⁹ the short-range order parameter for this problem, enters into the recursion relation for $\tilde{C}(\vec{q}, t)$ as part of the first-order correction. We can then consistently evaluate it at zeroth order where it obeys the recursion relation (4.5). We display the results for the iterated solution of (4.5) in Fig. 14 where we plot $\epsilon(1,0;t)$ as a function of time for various final temperatures. As expected this quantity grows initially more rapidly for deeper quenches. This is not as clear in the case of the lower-temperature quenches. In the inset we see that indeed, initially $\epsilon(1,0;t)$ grows more quickly after a quench to $u_F = 0.6$ than for the quench to $u_F = 0.5$. However, there is a crossover after a relatively short time. This corresponds physically to the situation where initially the system responds rapidly to set up a local equilibrium. The low-temperature quench, being further from equilibrium, will initially elicit a more vigorous response. After local order is achieved, one expects the lower-temperature system to respond

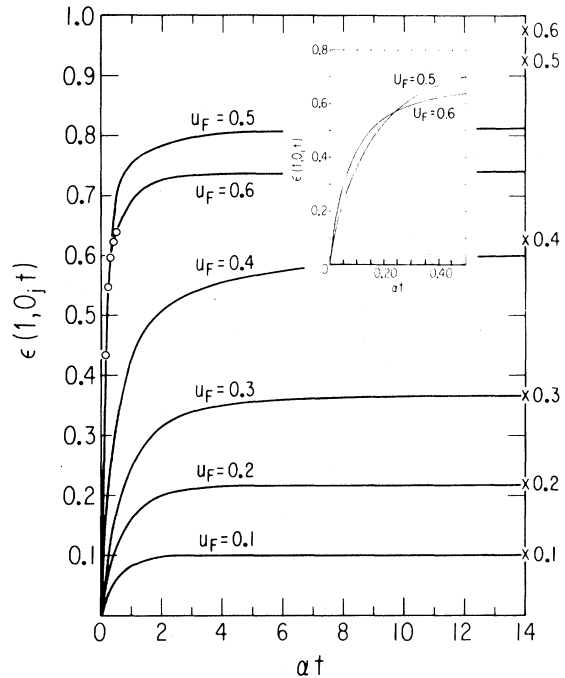


FIG. 14. Nearest-neighbor correlation function (short-range order parameter) vs αt at the indicated values of u_F . The crosses, labeled by u_F , indicate the corresponding final equilibrium values for $\epsilon(1,0;t)$. The open circles indicate the early time values of $\epsilon(1,0;t)$ for $u_F = 0.6$, which are shown more clearly in the inset.

more slowly since the domains will be more rigid at the lower temperature. It is useful to recall, here and in the rest of this section, the remark made below (2.7) in regard to the physical meaning of the expressions “early times” and “late times” as used here.

C. Analysis of $\tilde{C}(\vec{q}, t)$

The bulk of this section is devoted to the analysis of the solution of the recursion relation (4.17) for $\tilde{C}(\vec{q}, t)$. The only significant difference in numerically implementing the iterative solution of (4.51) and in our previous work^{9,35} is that $\tilde{C}(\vec{q}, t)$ couples to $H(\vec{q}, t)$. If, however, we introduce a vector, with components $\tilde{C}(\vec{q}, t)$ and $H(\vec{q}, t)$, we can rewrite our recursion relation in the standard form and continue as before. As explained in Sec. III, if $u_F > u_c$, the time eventually iterates to zero and the iterated $\tilde{C}(\vec{q}, t)$ flows to one.

The parameters characterizing $\tilde{C}(\vec{q}, t)$ are αt , u_I , u_F , and \vec{q} . We have chosen to present results only for the subspace $q_x = q_y$ and $u_I = 0$. While there are certain anisotropic effects in q space which may be studied, we have found them to be qualitatively less interesting and general than the results we present. The case of quenches for $u_I > 0$ is qualitatively the same as for $u_I = 0$ except if u_I begins to enter the critical region. Quenches from within the critical region will be discussed elsewhere.

In Fig. 4 we show $\tilde{C}(\vec{q}, t)$ for fixed $q_x = 0.02\pi$ and $u_F = 0.42$ as a function of time. We see that the structure pulse found when quenching within the disordered phase^{9,22} also occurs here. $\tilde{C}(\vec{q}, t)$ rises rather rapidly to a maximum value and then begins to decay rather slowly to its final equilibrium value. While this pulse structure is similar to that observed in the disordered case, it is complicated by a set of rather weak oscillations for intermediate times. This seems to indicate that there are really a series of pulses occurring when we quench into the unstable region. We see further evidence for this below.

We plot $\tilde{C}(\vec{q}, t)$ versus wave number⁴⁸ in Fig. 1 for various times and $u_F = 0.42$. The main features are the growth of the central peak, corresponding to domain formation, and the equilibration of large wave numbers. Inspection of these curves shows that there is some shape change in the central peak as time evolves. These changes of shape appear to be associated with the movement of pulses from high to low wave number as time evolves⁴⁹ (as in the shoulder for the case $\alpha t = 100$).

While our analytical development at the beginning of this section indicated that we have scaling at sufficiently long times and small wave numbers, we need to investigate the validity of scaling for finite

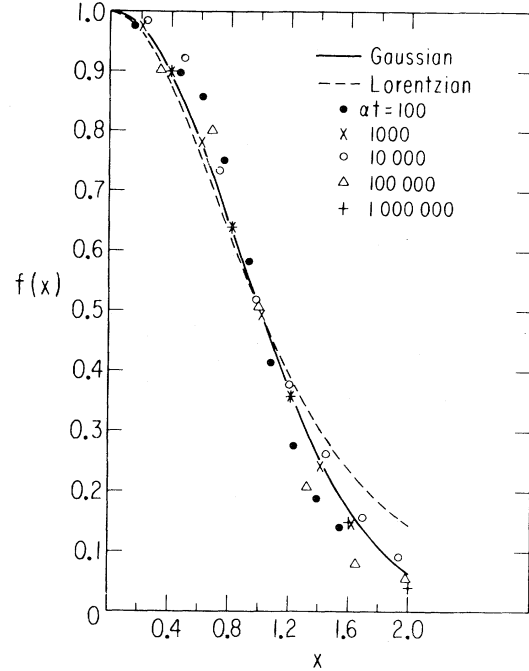


FIG. 15. We plot $f(x) = \tilde{C}(\vec{q}, t) / \tilde{C}(0, t)$ vs $x = q_x / q_w$ at the times indicated by the labels. The solid and dashed lines are Gaussian and Lorentzian fits (see text).

times and small wave numbers. In Fig. 15 we plot values of $\tilde{C}(\vec{q}, t) / \tilde{C}(0, t)$ vs $q / q_w(t)$, where $q_w(t)$ is the halfwidth at half maximum, for a number of times and for $u_F = 0.42$. For comparison we have also plotted Gaussian and Lorentzian fits to $\tilde{C}(\vec{q}, t)$. We have found that at many times (such as $\alpha t = 10^3$ and 10^6) the shape is well represented by a Gaussian, while for other times (such as $\alpha t = 10^2$ and 10^4) there is a change in shape which seems to represent a fluctuation about a Gaussian. The Lorentzian shape gives a poor fit for all times. We draw the conclusion that the shape of $\tilde{C}_p(\vec{q}, t)$, as a function of q , is roughly Gaussian.

In Sec. I we introduced the notion of an effective magnetization $M_E(t)$. We define this quantity more carefully here. First we must settle on a precise definition of $\tilde{C}_p(\vec{q}, t)$. One cannot define $\tilde{C}_p(\vec{q}, t) = \tilde{C}(\vec{q}, t) - \tilde{C}(\vec{q}, K_F)$ because this quantity has (except for long times) significant weight away from $q = 0$ and its integral over all q [given (5.13) and (5.14)] is trivially $m^2(K_F)$ and independent of time. A useful definition of $\tilde{C}_p(\vec{q}, t)$ restricts it to small wave numbers. We define

$$\tilde{C}_p(\vec{q}, t) = \Theta(\Lambda q_w(t) - q) [\tilde{C}(\vec{q}, t) - \tilde{C}(\vec{q}, K_F)], \quad (5.18)$$

where the step function restricts the magnitude of the wave number to magnitudes less than Λq_w . We

have chosen $\Lambda=2.5$ although the particular choice should not be very important. We then define

$$M_E^2(t) = \int \frac{d^2q}{(2\pi)^2} \tilde{C}_p(\vec{q}, t). \tag{5.19}$$

We plot $M_E^2(t)$ versus time in⁵⁰ Fig. 2 for $u_F=0.42$. We see that $M_E^2(t)$ is given accurately by $0.0091 \ln(at)$ for at between 1 and 100. For longer times $M_E^2(t)$ begins to saturate. There is some evidence for the pulses mentioned above near $at=10^5$ and 10^{10} .

If we return to the result that $\tilde{C}_p(\vec{q}, t)$ is roughly Gaussian, we can write

$$\tilde{C}_p(\vec{q}, t) \approx \frac{M_G^2(t)}{q_w^2(t)} f_G(\vec{q}/q_w), \tag{5.20}$$

where f_G is normalized⁵¹ as in (5.15) and given by

$$f_G(\vec{x}) = 2\pi(\ln 2) e^{-(\ln\sqrt{2})x^2}. \tag{5.21}$$

If we set $q=0$ in (5.20), we obtain the relationship⁵²

$$M_G^2(t) = \frac{\tilde{C}(0, t) q_w^2(t)}{2\pi \ln 2}. \tag{5.22}$$

In Fig. 2 the dots give $M_G^2(t)$ for the case $u_F=0.42$. The difference between $M_G^2(t)$ and $M_E^2(t)$ measures non-Gaussian corrections.

In Fig. 16 we plot $\tilde{C}(0, t)$ for several temperatures as a function of time. For early times $\tilde{C}(0, t)$ grows approximately with the power-law dependence $(at)^{1.5}$ for all three temperatures. In keeping with our discussion of $\epsilon(1, 0; t)$, we see that for short times the peak height for the lower temperature is larger than for the higher temperature. Eventually, as we explained before, we expect to obtain a crossover as it becomes progressively more difficult for the more ordered system to evolve.

In Fig. 3 we show q_w versus time for intermediate times and three final temperatures (corresponding to the final temperatures investigated in Ref. 20). We

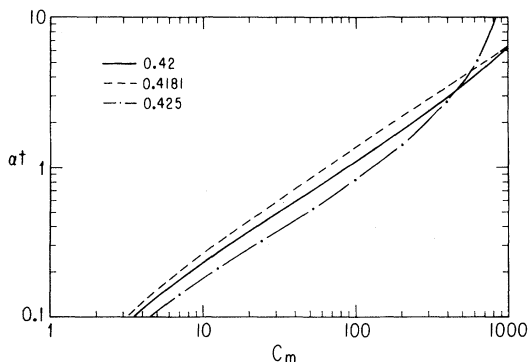


FIG. 16. Growth of $C_m = \tilde{C}(0, t)$ with time, at the labeled temperatures.

TABLE II. Values of the parameters characterizing q_w/π for intermediate times at three final temperatures.

u_F	β	t_0
0.4181	62.7	0.323
0.42	61	0.183
0.425	43.6	-0.182

obtain excellent root-mean-square fits for the time region $0.45 < at < 1.3$ to the form $q_w/\pi = \beta^{-1}(t - t_0)^{-1/2}$, where β and t_0 are given in Table II. As expected t_0 decreases with decreasing temperature. This corresponds to the fact that the local degrees of freedom, before there is any local constraining order, react more quickly to a deeper quench to set up a local equilibrium. Once this rather rapid equilibrium is established one has essentially a random distribution of domains. The deeper the quench the more difficult it will be for a domain to grow at the expense of its neighbors. There is, therefore, a crossover between the response of the local degrees of freedom at short times and the response of domains at longer times.

The long-time behavior of q_w vs $w = \log_{10}(at)$ is plotted in Fig. 17 at $u_F=0.42$. This figure shows the freezing behavior, mentioned previously, for large w . We see, for example, that q_w does not change appreciably for w between 12 and 20. Eventually as time increases the freeze ends and q_w again decreases until another freeze develops. We see in Fig. 17 that our results can be reasonably well fitted, allowing for the freeze, by the scaling result given by

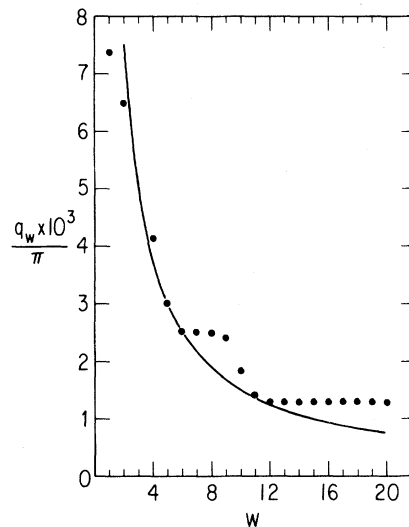


FIG. 17. Halfwidth at half maximum as a function of $w = \log_{10}(at)$. The dots are the results from the solution of (4.17) and the solid line is a fit to the long-time scaling result (5.11) with $q_0/\pi = 0.0346 \ln(y^{-1})$.

(5.11) with $q_0/\pi=0.0346\ln(y^{-1})$.

We plot in Fig. 5 the structure factor versus the final temperature for a series of times and for fixed $q_x=q_y=0.03\pi$. For short times we see that there is a single peak at a value of T_F below T_c . This is in agreement with the calculation in I where, for short times, no peak appears in the disordered region. Going to longer times ($\alpha t=10$) we see that the single peak splits into two peaks. The high-temperature peak clearly corresponds to that discussed in I. The second peak is associated with the development of the central peak in the “ordered” phase. Thus for $\alpha t=10$ and $u_F=0.45$ the large central peak encompasses $q_x=0.03\pi$, while for $u_F>0.60$ the peak is considerably smaller in intensity. Notice that the high-temperature peak is still located at a temperature below T_c . For $\alpha t=1000$ we see that the high-temperature peak has moved to a value greater than T_c . Notice that for a quench to very high temperature, $\bar{C}(\vec{q},t)$ has already equilibrated.

In characterizing the low-temperature peak we can define a “temperature” $u_p(t)$ such that for $u_F < u_p(t)$ the Fourier component of the structure factor under discussion has essentially equilibrated, while for $u_F > u_p(t)$ the component is still part of the central peak. We define u_p as the smaller value of u_F corresponding to the half maximum of the low-temperature peak. The approximate values of u_p are listed in Table III. We see that as time progresses the more shallow quenches equilibrate earlier. The transition between being in or out of equilibrium is very narrow as a function of u_F . While there is the development of structure in the low-temperature peak, it is not clear how seriously we should take the details of this structure.

VI. DISCUSSION

In this paper we have shown how the simple, physical ideas about self-similarity discussed in Sec.

TABLE III. For couplings $u > u_p$, at the times listed, the Fourier component $q_x=q_y=0.03\pi$ has equilibrated, while for $u < u_p$ the same Fourier component is still part of the central peak.

$u_p(t)$	αt
0.425	10
0.431	100
0.436	1000
0.438	10^4
0.443	10^5
0.448	10^6
0.465	10^{10}

III can be translated into a working mathematical formalism which, for the model under consideration, allows the evaluation of the structure factor of the system in the case of a deep temperature quench. Thus, we have been able to study the growth of order in the system. We believe that our results, presented in the preceding section, give a good description of the main physical features of the problem. We now discuss some possible improvements, which emerge rather naturally out of the present calculation, as well as some possible extensions and generalizations.

Note first, while it is true that some parts of the present calculation are quite complicated, that this is primarily due to our present need to evaluate the recursion relations to first order. This is a technical, not a fundamental, point which may well be overcome in the future. Conceptually the method is quite simple. The new fundamental insight is the careful study of the time rescaling factor $\Delta(K)$ (Appendix A) which leads to the parameter flows found in Sec. III. It is the qualitative behavior of these flows that is really at the heart of the matter.

A second point, which at first sight appears technical but which has physical ramifications, is the treatment of the quantity $R[\mu,t]$, defined by (4.14), which is reflected in the quantity $H(\vec{q},t)$ appearing in the recursion relation for $\bar{C}(\vec{q},t)$, (4.17). An alternative approach, which we believe is feasible and which avoids these complications, is to assume that after renormalization the new final coupling K_F is time dependent in such a manner that $R[\mu,t]=1$. We expect, however, that this time dependence will be relatively weak. The occurrence of a time-dependent K_F should, however, not be too surprising since this is just what one would have if finite quench rates were included. We will discuss this interesting situation elsewhere.

As we pointed out, one of our results in the last section is probably not realistic. This is the freezing and unfreezing feature occurring for very long times. We believe that this effect can be understood if we recognize that in our calculation we have kept track of only the slowest local mode $\psi_i^{(1)}$ under renormalization. This mode is associated with the local Ising block spin. For many purposes this picture seems adequate. We believe it properly describes the slowest processes in the system and the buildup of local order. However, we do not believe that this picture leads to a convenient description of the fluctuations in the system at low temperatures. This is reflected in the difficulties associated with the zeroth-order calculation of the equilibrium susceptibility [see the discussion below (4.10)], which are not found when calculating the magnetization. The problem is that the low-temperature fluctuations in

the system are associated with domain walls and it is difficult to treat the motion of domain walls within the rigid block-spin picture. Indeed, after several coarse-graining iterations, the block-spin dynamics, flipping of domains, becomes so slow that it is almost impossible for them to flip on reasonable time scales, and they freeze. There are, however, other degrees of freedom which will, as things slow down under progressive renormalization, become important on the time scales of interest. The obvious candidates in this case are vacancies (or lines of vacancies forming domain walls). In carrying out a renormalization including vacancies we must introduce an additional set of variables to monitor vacancies which will have their own associated relaxation rate. We expect this relaxation rate to be faster than that associated with domain flipping at low temperatures and to represent the important long-time thermalizing agents. From a physical point of view this means that we obtain a more accurate representation of the self-similarity in the problem if we allow for the occurrence of vacancies in our coarse graining. Inclusion of vacancies into our formalism is not difficult and is currently under investigation.

We believe that the present work opens up the possibility of studying the growth of order in a number of different models. The problem of spinodal decomposition is the most obvious candidate since it can be studied by means of a kinetic Ising model with a conserved order parameter. We are currently addressing this and related questions.

ACKNOWLEDGMENTS

This work was supported by NSF Grant No. DMR80-20609, by the University of Minnesota Graduate School Research Fund, and the MEIS center. One of us (G.F.M.) thanks Professor J. Hertz and NORDITA, Professor W. Kohn and the Institute for Theoretical Physics at the University of California at Santa Barbara, and Professor W. Weyhmann and Professor A. Goldman at the University of Minnesota for their support and hospitality during visits where parts of this research were carried out. We thank Professor J. Langer and Professor J. Hirsch for useful discussions on this work. We also thank Dr. P. Sahni for assistance with Fig. 6 and Professor T. Eguchi for permission to use a figure from Ref. 41.

APPENDIX A: THE TIME-RENORMALIZATION FACTOR

As discussed below (3.10) the time rescaling factor $\Delta(K)$ must be obtained from the recursion relation for the equilibrium dynamic structure factor $C(\vec{q}, z)$. At long wavelengths and low frequencies, this recur-

sion relation is given by (4.13a) of Ref. 35 as follows:

$$C(0,0) = \frac{4v_1^2}{\Delta} C'(0,0) + O(\epsilon). \quad (\text{A1})$$

Upon writing

$$C(\vec{q}, z) = \tilde{C}(\vec{q}, K) / [z + i\alpha\phi(\vec{q}, z)],$$

where ϕ is the associated memory function,⁵³ we obtain the result

$$\Delta = 4v_1^2 \frac{\chi' \phi(0,0)}{\chi \phi'(0,0)}, \quad (\text{A2})$$

where $\chi = \tilde{C}(0, K)$ is the susceptibility. The memory function ϕ can be written as the sum

$$\phi(0,0) = (\Gamma^{(s)} + \Gamma^{(d)}) \chi^{-1}, \quad (\text{A3})$$

where

$$\Gamma^{(s)} = 1 - 2a(K)\epsilon(1,0) + a^2(K)\epsilon(1,1), \quad (\text{A4})$$

and the formal definition of $\Gamma^{(d)}$ is given by (3.4) in Ref. 53. We know several things, however, about $\Gamma^{(d)}$. First⁵³

$$\Gamma^{(s)} \geq |\Gamma^{(d)}| \quad (\text{A5})$$

for all temperatures, next

$$\left| \frac{\Gamma^{(d)}}{\Gamma^{(s)}} \right| = \frac{4}{3} u^4 + O(u^5) \quad (\text{A6})$$

for high temperatures, and finally

$$\left| \frac{\Gamma^{(d)}}{\Gamma^{(s)}} \right| \sim O(y^2) \quad (\text{A7})$$

for low temperatures ($y = e^{-4K}$). It seems very reasonable to neglect $\Gamma^{(d)}$ as a first approximation. An immediate consequence of this result is that one obtains a dynamic critical index z given by its conventional value $z = \gamma = 1.76$. As we pointed out elsewhere⁵³ this should be a good approximation over most of the critical region except for temperatures very close to T_c . A recent neutron scattering experiment³⁶ has confirmed this result. Substitution of $\phi = \Gamma^{(s)} \chi^{-1}$ into (A2) leads to the result (3.11) for Δ .

Note, for $T > T_c$, we can, to a good approximation, use the zeroth-order recursion relation $\chi = 4v_1^2 \chi'$ in (A3) and obtain

$$\Delta = \Gamma^{(s)}(K) \chi' / \Gamma^{(s)}(K') \chi,$$

which we used in Ref. 34. It was inappropriately used in Ref. 45 where we should have used (3.11).

APPENDIX B: SINGLE-CELL AVERAGES

There are three independent zeroth-order time-dependent averages, namely,

$$r(t) = \sum_{\sigma}^i \sigma_a \sigma_{a+1} P_0^i[\sigma, t], \quad (\text{B1})$$

$$s(t) = \sum_{\sigma}^i \sigma_a \sigma_{a+2} P_0^i[\sigma, t], \quad (\text{B2})$$

$$v(t) = \sum_{\sigma}^i \sigma_a \sigma_{a+1} \sigma_{a+2} \sigma_{a-1} P_0^i[\sigma, t]. \quad (\text{B3})$$

These averages are easily calculated by expanding $P_0^i[\sigma, t]$ in terms of the eigenfunctions³⁴ of $\tilde{D}_{\sigma}^0(K_F)$ as follows:

$$P_0^i = \sum_l e^{-\lambda_{F,l}^i t} \psi_i^{(l)}(\sigma, K_F) P_0^i[\sigma, K_F] \times \sum_{\sigma'} \psi_i^{(l)}(\sigma', K_F) P_0^i[\sigma, K_I]. \quad (\text{B4})$$

Only the even, uniform eigenfunctions contribute to the averages, and thus one obtains the results

$$r(t) = r_F + \frac{1}{2} \sum_{l=\pm} e^{-E_{l,F} \tau} \left[r_I - r_F + l \frac{\sqrt{2}}{2} (s_I - s_F) \right], \quad (\text{B5a})$$

$$s(t) = s_F + \frac{1}{2} \sum_{l=\pm} e^{-E_{l,F} \tau} [-l\sqrt{2}(r_I - r_F) + (s_I - s_F)], \quad (\text{B5b})$$

$$v(t) = s_F + \sum_{l=\pm} e^{-E_{l,F} \tau} [-a_{0,F} + 2r_I - a_{0,F} s_I + l\sqrt{2}(s_I - a_{0,F} r_I)] - e^{-4\tau} (4r_F r_I - 2s_F s_I - s_F - s_I), \quad (\text{B5c})$$

$$E_{l,F} = 2 - \sqrt{2} a_{0,F} l, \quad (\text{B5d})$$

$$\tau = \alpha_{0,F} t, \quad (\text{B5e})$$

where r_I , r_F , s_I , and s_F are the corresponding equilibrium values for $r(t)$ and $s(t)$.

¹The temperature here refers to that of a ‘‘bath’’ in which the system is immersed and with which it is initially in thermal equilibrium.

²The case where there are more than two competing degenerate ground states can lead to slower long-time equilibration mechanisms. See, for example, S. Safran, *Phys. Rev. Lett.* **46**, 1581 (1981).

³In most practical cases there will be various mechanisms (crystal imperfections, finite size, etc.) cutting off the growth.

⁴A. Guth and P. Steinhardt, private communications. See for example, A. Guth, *Proceedings of the Second Moriond Astrophysics Meeting* (unpublished).

⁵The recent review by J. Gunton, M. San Miguel, and P. Sahni (unpublished), gives a rather complete introduction to the literature.

⁶C. Billotet and K. Binder, *Z. Phys. B* **32**, 195 (1979).

⁷K. G. Wilson, *Rev. Mod. Phys.* **47**, 773 (1975).

⁸Of course, in a real ferromagnet the conjugate field is never strictly zero. However, our results for the square lattice are equivalent, by a trivial translation of the vectors, to results for the antiferromagnetic case where the assumption of zero field is realistic.

⁹G. F. Mazenko, *Phys. Rev. B* **26**, 5103 (1982). This paper will be referred to as I and equations labeled (I.XXX) refer to this paper.

¹⁰This result can be found from a perturbation-theory

analysis of the time-dependent Ginzburg-Landau equation in the case where one quenches in temperature and turns off a magnetic field, H , at some time $t_0=0$. If one then takes the limit $H \rightarrow 0$, one obtains (1.1) for any finite time. If, however, one takes the limit $t \rightarrow \infty$ first, then $H \rightarrow 0$, one obtains the usual equilibrium value for the spontaneous magnetization.

¹¹K. Kawasaki, M. Yalabik, and J. Gunton, *Phys. Rev. A* **17**, 455 (1978).

¹²J. W. Cahn and S. M. Allen, *J. Phys. (Paris) Colloq.* **C7**, 54 (1977); S. M. Allen and J. W. Cahn, *Acta Metall.* **27**, 1085 (1979).

¹³In Ref. 12, L^{-1} is associated with the square root of the surface area per unit volume and t_0 is associated with an integration constant [see their Eq. (24)].

¹⁴S. Chan, *J. Chem. Phys.* **67**, 5755 (1977).

¹⁵M. San Miguel, J. Gunton, G. Dee, and P. S. Sahni, *Phys. Rev. B* **23**, 2334 (1981).

¹⁶K. Kawasaki and T. Ohta, *Prog. Theor. Phys.* **67**, 147 (1982).

¹⁷C. Kawabata and K. Kawasaki, *Phys. Lett.* **65A**, 137 (1978).

¹⁸M. K. Phani, J. L. Lebowitz, M. H. Kalos, and O. Penrose, *Phys. Rev. Lett.* **45**, 366 (1980).

¹⁹P. S. Sahni, G. Dee, J. Gunton, M. Phani, J. Lebowitz, and M. Kalos, *Phys. Rev. B* **24**, 410 (1981).

²⁰T. Hashimoto, K. Nishimura, and Y. Takeuchi, *Phys.*

- Let. 65A, 250 (1978).
- ²¹Analysis and references to a large number of studies of the time dependence of domain coarsening are given in Allen and Cahn, Ref. 12.
- ²²G. F. Mazenko and M. Widom, Phys. Rev. B 25, 1860 (1982).
- ²³K. Binder, Phys. Rev. B 8, 3423 (1973).
- ²⁴See J. S. Langer, M. Bar-on, and H. D. Miller, Phys. Rev. A 11, 1417 (1975), and references therein to earlier work.
- ²⁵K. Kawasaki, Phys. Rev. 145, 224 (1966); 148, 375 (1966); 150, 285 (1966); K. Kawasaki, in *Phase Transitions and Critical Phenomena*, edited by C. Domb and M. S. Green (Academic, New York, 1972), Vol. 2.
- ²⁶R. J. Glauber, J. Math. Phys. (N.Y.) 4, 294 (1963).
- ²⁷This should be unimportant for quenching temperatures $T_F \lesssim T_c$, but it could be significant if $T_F \ll T_c$, which is the region studied in Ref. 17 ($u_F = \tanh K_F = 0.9759$).
- ²⁸J. Hirsch, private communication.
- ²⁹C. N. Yang, Phys. Rev. 85, 808 (1952).
- ³⁰B. Kaufmann and L. Onsager, Phys. Rev. 76, 1244 (1949).
- ³¹C. Domb, in *Phase Transitions and Critical Phenomena*, edited by C. Domb and M. S. Green (Academic, New York, 1974), Vol. 3.
- ³²M. Fisher and R. Burford, Phys. Rev. 156, 583 (1967).
- ³³H. Tarko and M. Fisher, Phys. Rev. B 11, 1217 (1975).
- ³⁴G. F. Mazenko and O. T. Valls, Phys. Rev. B 24, 1404 (1981).
- ³⁵G. F. Mazenko and O. T. Valls, in *Real Space Renormalization*, edited by J. M. J. van Leeuwen and T. W. Burkhardt (Springer, Berlin, 1982).
- ³⁶M. T. Hutchings, H. Ikeda, and E. Janke, Phys. Rev. Lett. 49, 386 (1982).
- ³⁷M. Collins and H. Teh, Phys. Rev. Lett. 30, 781 (1973); T. Hashimoto, T. Miyoshi, and H. Ohtsuka, Phys. Rev. B 13, 1119 (1976).
- ³⁸Some of the general properties of this and related operators is discussed in G. F. Mazenko, M. J. Nolan, and O. T. Valls, Phys. Rev. B 22, 1263 (1980). Note that we adopt the notation $D_{\sigma} A[\sigma] = \sum_{\sigma'} D[\sigma | \sigma'] A[\sigma']$.
- ³⁹This point is discussed in Sec. II A of Ref. 5 and in Ref. 37.
- ⁴⁰See, for example, K. Binder and M. H. Kalos, in *Monte Carlo Methods in Statistical Physics*, edited by K. Binder (Springer, Berlin, 1979).
- ⁴¹K. Oki, H. Sagana, and T. Eguchi, J. Phys. (Paris) C7, 414 (1977).
- ⁴²G. F. Mazenko, J. Hirsch, M. J. Nolan, and O. T. Valls, Phys. Rev. B 23, 1431 (1981).
- ⁴³A detailed discussion is given for the one-dimensional case in G. F. Mazenko and J. Luscombe, Ann. Phys. (N.Y.) 132, 121 (1981).
- ⁴⁴G. F. Mazenko, in *Dynamic Critical Phenomena and Related Topics*, edited by C. P. Enz (Springer, Berlin, 1979).
- ⁴⁵G. F. Mazenko and O. T. Valls, Phys. Rev. B 26, 389 (1982).
- ⁴⁶For technical reasons it is also useful to introduce the first-order parameter δa_1 corresponding to a small shift in a_0 and a parameter C corresponding to a rotation in μ space (as described by J. Luscombe and G. Mazenko, Ann. Phys. (N.Y.) (in press). These additional parameters and a_R are completely determined by demanding that (i) the recursion relation (3.9) holds to first order, (ii) that the equilibrium version of the recursion relation for $\epsilon(1,0)$ given by (4.5) and determining a_0 , hold also at first order (thus the first-order correction must vanish), and (iii) that the coefficient χ' in the recursion relation for χ (the susceptibility) lead to the correct asymptotic behavior for χ in the high- and low-temperature limits. The parameters δa_1 and C , so determined, indeed turn out to be small in magnitude (< 0.036) over the entire temperature range.
- ⁴⁷This occurs because the zeroth-order theory gives the correct leading low-temperature behavior for all of the observables.
- ⁴⁸Henceforth we measure all wave numbers in units of c^{-1} (i.e., $\vec{q}c \rightarrow \vec{q}$).
- ⁴⁹A similar effect seems to be present in P. S. Sahni and J. Gunton, Phys. Rev. Lett. 45, 369 (1980). See Fig. 2.
- ⁵⁰In carrying out this analysis we have assumed that $\tilde{C}_p(\vec{q}, t)$ is isotropic.
- ⁵¹It leads to a very small error if we extend the limits of integration to infinity.
- ⁵²The difference between $\tilde{C}(0, t)$ and $\tilde{C}(\cdot, t) - \tilde{C}(0, K_F)$ is insignificant for all but the earliest times.
- ⁵³G. F. Mazenko and O. T. Valls, Phys. Rev. B 24, 1419 (1981).

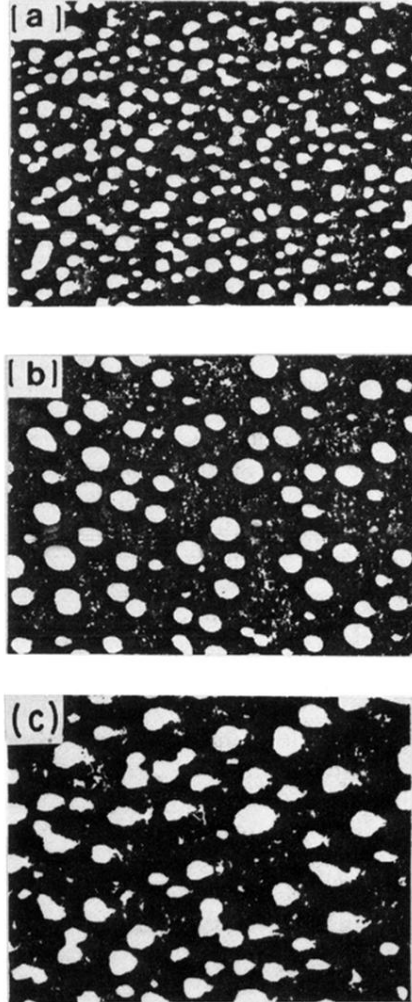


FIG. 6. Domain structures imaged (Ref. 41) with B_2 superlattice reflection in 23.0 at. % Al in Fe alloy. The samples were quenched from 630°C and annealed at 570°C. In panel (a) the system was annealed for 100 min while in panel (b) it was annealed for 1000 min. In panel (c) we have taken a portion of panel (a) with approximately the same number of domains as in panel (b) and then blown this portion up to the same size as panels (a) and (b). Comparison of panels (b) and (c) illustrates the self-similar structure of the system under simultaneous rescalings of space and time.